

The author would like to thank Professor M. O'Keeffe, Arizona State University, for supplying the crystal and reading the manuscript. He also thanks Drs P. Goodman and J. W. Steeds for valuable discussions. The work was supported by NSF grants DMR80-15785 and by the Facility for High-Resolution Electron Microscopy, established with the support by NSF Regional Instrumentation Facilities Program (CHE-791608).

References

BANDO, Y., SEKIKAWA, Y., YAMAMURA, H. & MATSUI, Y. (1981). *Acta Cryst.* **A37**, 723–728.

BUXTON, B. F., EADES, J. A., STEEDS, J. W. & RACKHAM, G. M. (1976). *Philos. Trans. R. Soc. London Ser. A*, **281**, 171–194.
 GJØNNES, J. & MOODIE, A. F. (1965). *Acta Cryst.* **19**, 65–67.
 GOODMAN, P. (1975). *Acta Cryst.* **A31**, 804–810.
 GOODMAN, P. & O'KEEFFE, M. (1980). *Acta Cryst.* **B36**, 2891–2893.
 GRÜN, R. (1979). *Acta Cryst.* **B35**, 800–804.
 JOHNSON, A. W. S. & GATEHOUSE, B. M. (1980). *Acta Cryst.* **B36**, 523–526.
 KATO, K., INOUE, Z., KIJIMA, K., KAWADA, I. & TANAKA, H. (1975). *J. Am. Ceram. Soc.* **58**, 90–91.
 TANAKA, M., SAITO, R. & WATANABE, D. (1980). *Acta Cryst.* **A36**, 350–352.
 WILD, S., GRIEVESON, P. & JACK, K. H. (1972). *Spec. Ceram.* **5**, 385–393.

Acta Cryst. (1983). **B39**, 189–197

The Structure of Potassium-Exchanged Heulandite at 293, 373 and 593 K

BY E. GALLI AND G. GOTTARDI

Istituto di Mineralogia e Petrologia dell'Università, Via S. Eufemia 19, I-41100 Modena, Italy

H. MAYER AND A. PREISINGER

Institut für Mineralogie, Kristallographie und Strukturchemie, Technische Universität Wien, Getreidermarkt 9, A-1060 Wien, Austria

AND E. PASSAGLIA

Istituto di Mineralogia dell'Università, C. so Ercole I° d'Este 32, I-44100 Ferrara, Italy

(Received 28 June 1982; accepted 13 October 1982)

Abstract

Single crystals of heulandite (Mossyrock Dam, Lewis County, Washington, USA) were potassium-exchanged to reach a chemical composition of $(\text{Na}_{0.10}\text{K}_{8.57}\text{Ba}_{0.04})(\text{Al}_{9.31}\text{Si}_{26.83})\text{O}_{72}\cdot 19\cdot 56\text{H}_2\text{O}$. Thermogravimetry up to 593 K of such single crystals was carried out concurrently with the X-ray diffraction measurements of one single crystal at 293, 373 and 593 K. At 593 K the sample was fully dehydrated. The crystal structures were refined by least squares to R_w values of 0.073 (293 K), 0.090 (373 K) and 0.112 (593 K). [Crystal data for the first structure (293 K): $C2/m$, $a = 17.767$ (7), $b = 17.958$ (7), $c = 7.431$ (1) Å, $\beta = 115.93$ (2)°.] The crystal structure at 593 K is essentially in agreement with that at 293 K of a single crystal previously heated to 573 K in an evacuated and sealed glass capillary. The process of dehydration is represented by these crystal structure determinations

showing the change of the water molecules and the positions of the K^+ ions as well as the deformation of the silicate framework.

Introduction

It is a common practice to study the structures of dehydrated zeolites by sealing in glass capillaries crystals previously dehydrated in vacuum at high temperatures. The first aim of the present study is to check if any meaningful difference exists between the structure of a zeolite at 593 K and the structure of the same zeolite at 293 K after heating in vacuum at 573 K and sealing in a glass capillary. The second aim is to compare the hydrated structure at room temperature with the partially dehydrated structure at 373 K and the dehydrated structure at 593 K in order to detect which water molecule leaves first, and how cations change sites with increasing temperature.

Table 1. *Crystal and experimental data of K-exchanged heulandite*

Data-collection conditions: (I) at 293 K; (II) at 373 K; (III) at 593 K; (IV) at 293 K after heating in vacuum at 573 K and sealing in a glass capillary.

Unit-cell contents from the chemical analysis: $(\text{Na}_{0.10}\text{K}_{8.57}\text{Ba}_{0.04})(\text{Al}_{9.31}\text{Si}_{26.83})\text{O}_{72} \cdot 19.56\text{H}_2\text{O}$.

	(I)	(II)	(III)	(IV)
<i>a</i> (Å)	17.767 (7)	17.727 (17)	17.536 (8)	17.480 (10)
<i>b</i> (Å)	17.958 (7)	17.733 (15)	17.277 (5)	17.340 (10)
<i>c</i> (Å)	7.431 (1)	7.434 (2)	7.409 (1)	7.407 (5)
β (°)	115.93 (2)	116.47 (4)	116.62 (2)	116.33 (4)
Volume (Å ³)	2132 (1)	2092 (3)	2007 (1)	2012 (2)
Space group	<i>C2/m</i>	<i>C2/m</i>	<i>C2/m</i>	<i>C2/m</i>
Crystal size (mm)	0.11 × 0.19 × 0.35	0.11 × 0.19 × 0.35	0.11 × 0.19 × 0.35	0.12 × 0.24 × 0.35
Radiation (graphite-monochromated)	Mo <i>K</i> α	Mo <i>K</i> α	Mo <i>K</i> α	Mo <i>K</i> α
Scan type	ω -2 θ	ω -2 θ	ω -2 θ	ω -2 θ
Maximum θ (°)	25	25	25	30
ω scan speed (° s ⁻¹)	0.0333	0.0333	0.0333	0.1
ω scan width (°)	1.20	1.20	1.20	2.0
Time for each background (s)	40	40	40	5
Number of measured reflections	4231	4128	4008	5876
Number of independent reflections	1946	1907	1847	3045
Observed reflections [$I \geq 3\sigma(I)$]	1631	1569	1276	2419
Final isotropic <i>R</i> (including unobs.)	0.097	0.118	0.177	0.136
Final isotropic <i>R</i> (omitting unobs.)	0.085	0.103	0.143	0.115
Final isotropic <i>R</i> _w (omitting unobs.)	0.073	0.090	0.112	0.078

Experimental

Heulandite from Mossyrock Dam, Lewis County, Washington, USA, was used for this study. For two months a set of crystals whose average size was between 0.2 and 0.5 mm was treated in an aqueous NaCl solution in a Teflon reactor slowly oscillating in an oven at 383 K. The Na-exchanged form thus obtained was subsequently K-exchanged under similar conditions. The homogeneity of the K-exchanged crystals was checked by microprobe analyses (Passaglia, Pongiluppi & Vezzalini, 1978). The water content was determined by thermogravimetry.

Cell parameters and reflection intensities were measured on a Philips PW 1100 four-circle diffractometer with graphite-monochromatized Mo *K*α radiation. Data sets (I), (II) and (III) were obtained subsequently with the same crystal at 293, 373 and 593 K, set (IV) on a sealed crystal at room temperature. In the following, the results obtained under the four different conditions are coded (I), (II), (III) and (IV) according to Table 1.

For the high-temperature studies a heating device for single crystals, developed and partly constructed at the Institut für Mineralogie, Kristallographie und Strukturchemie der Technischen Universität Wien, was used.

The crystal was attached to a glass capillary by means of a temperature-resisting glue and was then heated to the required temperature on the usual goniometer head of the Philips PW 1100 instrument by using a hot-nitrogen stream of 2–3 mm diameter. The temperature stability proved to be better than 1 K. Nitrogen (99.99% N₂) was supplied *via* a fine reducing

valve through a corundum tube of 30 cm length with a heating spiral inside. The nitrogen served both as heating gas and as a protection of the heating spiral. To protect the four-circle diffractometer against thermal radiation, the corundum tube was inserted into a double-wall, gold-coated, evacuated SiO₂-glass tube. In addition a screening sheet and a thermofuse to protect against overheating were installed. The heating performance was electronically controlled *via* a thermoelement which was inserted into the gas stream directly in front of the crystal. The actual temperatures at the crystal were determined by corresponding calibration with a quartz crystal.

Fig. 1(a) shows the temperature/time diagram of this study, the lattice parameters of sets (I), (II) and (III) and those of the crystal cooled to 473 and 373 K. To simulate the dehydration behaviour of the single crystal during this X-ray study (Fig. 1a), a thermogravimetric curve with approximately the same temperature/time program was recorded on a METTLER thermoanalyser (Fig. 1b). The study was made under streaming nitrogen (99.999% N₂, flow rate 5 litre h⁻¹). The thermogravimetric temperature/time diagram shows that at 373 K after an isothermal temperature march of 8 h constant weight resulted; only after 50 h – the time required for the data collection at 373 K – was the loss of weight between 10.0 and 10.8 mol H₂O. At 593 K and at an isothermal march of temperature of 148 h the weight loss is between 18.47 and 18.87 mol H₂O, corresponding to the data collection at 593 K.

To determine any residual H₂O content, the sample was heated from 593 to 1173 K at 2 K min⁻¹. Under these conditions constant weight was noted at about 1073 K; the residual loss of weight corresponds to 0.69

mol H₂O. The result is given in Fig. 1(b). The crystals remaining after the thermal study were preserved in air at room temperature. After about 3 months the lattice parameters were determined for several of these single

crystals ($a = 17.782$, $b = 17.926$, $c = 7.435$ Å, $\beta = 115.91^\circ$) and the results correspond very well to those obtained with the originally unheated sample.

Structure refinements and results

The atomic parameters of natural clinoptililite (Alberti, 1975) were used as starting values for the refinements, which were carried out by alternating least-squares cycles (*ORFLS*, Busing, Martin & Levy, 1962) and difference electron density maps. The scattering functions for neutral atoms of Hanson, Herman, Lea & Skillman (1964) were used except for water, for which Hajdú's (1972) function was applied. Isotropic temperature factors only were applied. In the final stages of the least-squares refinements, occupancy factors and temperature factors were alternately varied in order to improve convergence. The atoms of the framework were named $T(1 \dots 5)$ and $O(1 \dots 10)$, while the extra-framework ones were named with numbers from 1 to 10, or by the same numbers in parentheses preceded by the symbol of the atom attributed to that site [*i.e.* 1 or K(1), 7 or K(7)...]. In the refinements (I) and (II) the extra-framework sites were assigned to water molecules or to K⁺ ions according to the following criteria: (a) maximum electron density in the site; (b) distances from the site to neighbouring framework O atoms and to other extra-framework sites; (c) reduction of the total electron density in one and the same site with increasing temperature was

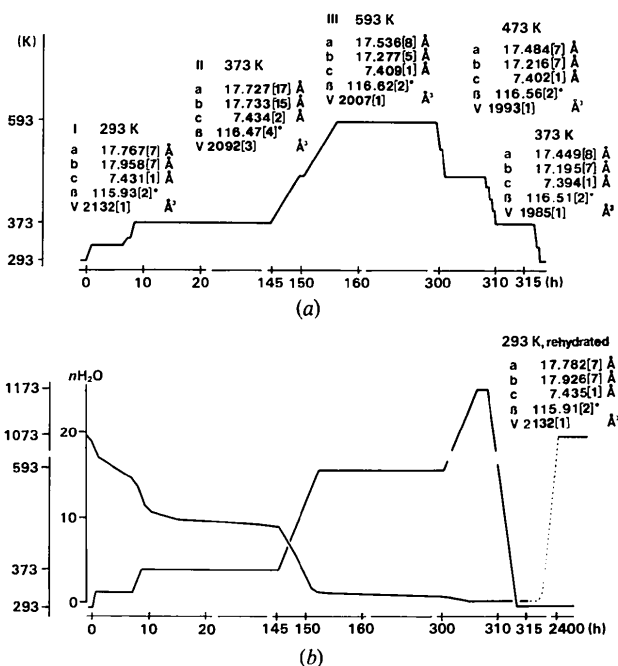


Fig. 1. Heating diagrams of K-exchanged heulandite. Temperature (K) versus time (h) diagrams for (a) X-ray diffraction and (b) thermogravimetry.

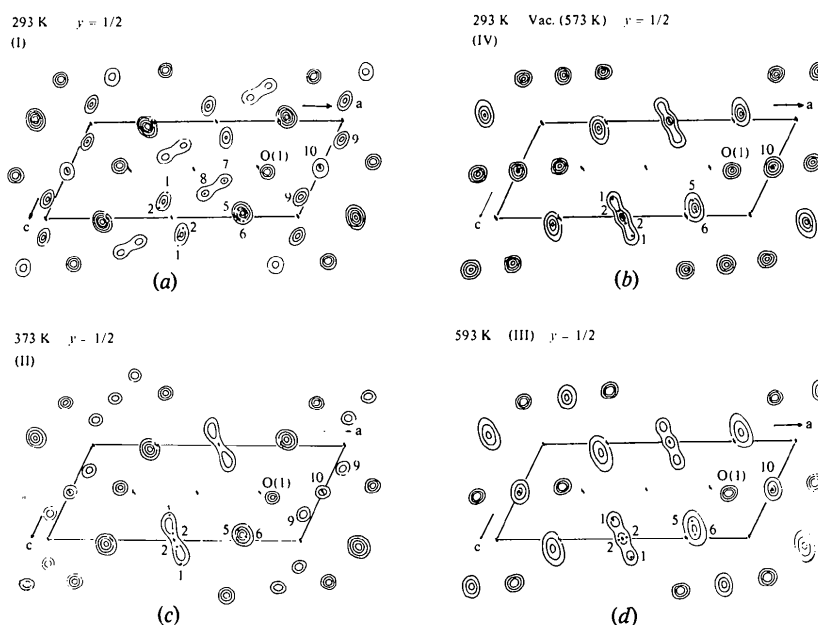


Fig. 2. Electron density maps of the Fourier section at $y = \frac{1}{2}$. O(1) and the extra-framework atom positions with $y = \frac{1}{2}$ are given.

considered as evidence for its occupancy by water. In sets (III) and (IV) all extra-framework sites (1 + 2, 5 + 6 and 10) were assigned to K⁺.

In all four sets (I, II, III and IV) the sites 1 + 2 as well as 5 + 6 are allocated to K⁺ ions. These sites are represented in the Fourier sections (Fig. 2a-d) by considerably smeared out peaks. Different models of calculations showed that the most appropriate way to describe each of these peaks is by a pair of split positions (1 + 2) and (5 + 6). This model should be

interpreted as 'coupled pairs' of statistically distributed K⁺ ions. The nearest neighbouring sites (1 + 2) cannot be occupied simultaneously because they are too close to each other; thus the statistical occupancy factors, using the scattering function of potassium, refined to a sum lower than 100% (70% in I and 50% in II, III and IV), giving very high *B* values. In refinements with a water curve the sum of the occupancy factors would rise decidedly above 100%, which is impossible. The higher occupancy factor of (1 + 2) in the fully hydrated

Table 2. *Positional parameters* ($\times 10^4$ for Si and O, and $\times 10^3$ for extra-framework sites), *isotropic temperature factors* (\AA^2) and *occupancy factors* (%), with their *e.s.d.*'s in parentheses, for K-exchanged heulandite

Sites 1, 2, 5, 6 and 9 are always occupied by K, and hence coded also as K(1), K(2) ... K(9); sites 3, 4, 7 and 8 are always occupied by H₂O, and hence coded also W(3) ... W(8). Site 10 was calculated for (I) and (II) as H₂O, and for (III) and (IV) as K.

Site		(I)	(II)	(III)	(IV)	Site		(I)	(II)	(III)	(IV)
T(1)	x	1794 (1)	1793 (2)	1796 (3)	1804 (1)	1	Occ.	34 (1)	30 (1)	29 (1)	23 (1)
8(j)	y	1686 (1)	1662 (2)	1606 (3)	1602 (1)	4(i)	x	79 (2)	76 (2)	74 (2)	77 (1)
	z	978 (3)	958 (4)	889 (8)	870 (3)		y	0	0	0	0
	B	1.0 (1)	1.4 (1)	2.3 (1)	1.4 (1)		z	281 (6)	260 (6)	195 (6)	191 (2)
T(2)	x	2146 (1)	2122 (2)	1939 (3)	1905 (1)		B	19.1 (11)	23.4 (20)	11.6 (11)	5.5 (3)
8(j)	y	4108 (1)	4110 (2)	4101 (3)	4099 (1)	2	Occ.	36 (1)	18 (1)	24 (1)	29 (1)
	z	5063 (3)	5015 (5)	4926 (7)	4990 (3)	4(i)	x	71 (1)	22 (3)	-15 (6)	19 (1)
	B	1.1 (1)	1.6 (1)	2.4 (1)	1.5 (1)		y	0	0	0	0
T(3)	x	2083 (1)	2075 (2)	2256 (3)	2292 (1)		z	110 (4)	78 (7)	22 (16)	58 (2)
8(j)	y	1912 (1)	1898 (2)	1827 (3)	1808 (1)		B	10.6 (6)	12.0 (10)	16.7 (21)	5.8 (3)
	z	7161 (3)	7186 (4)	7388 (7)	7384 (3)	3	Occ.	100	49 (2)		
	B	1.0 (1)	1.5 (1)	2.6 (1)	1.5 (1)	8(j)	x	408 (1)	441 (2)		
T(4)	x	668 (1)	652 (2)	694 (3)	712 (1)		y	92 (1)	83 (2)		
8(j)	y	2983 (1)	2967 (2)	2767 (3)	2720 (1)		z	49 (1)	35 (4)		
	z	4176 (3)	4166 (4)	4252 (7)	4267 (3)		B	9.7 (3)	17.4 (13)		
	B	1.1 (4)	1.6 (1)	2.3 (1)	1.3 (1)	4	Occ.	50	50 (1)		
T(5)	x	0	0	0	0	8(j)	x	8 (1)	12 (2)		
4(g)	y	2173 (2)	2147 (2)	1966 (4)	2002 (1)		y	99 (1)	90 (1)		
	z	0	0	0	0		z	414 (2)	378 (4)		
	B	1.3 (1)	1.5 (1)	2.2 (1)	1.5 (1)		B	8.0 (5)	12.8 (9)		
O(1)	x	1981 (5)	1902 (6)	1655 (9)	1580 (4)	5	Occ.	74 (1)	28 (2)	33 (1)	25 (1)
4(i)	y	↓	↓	↓	↓	4(i)	x	241 (1)	268 (2)	272 (2)	261 (1)
	z	4565 (12)	4421 (16)	4568 (23)	4658 (10)		y	↓	↓	↓	↓
	B	2.3 (2)	3.2 (2)	3.6 (4)	3.0 (1)		z	61 (1)	99 (4)	175 (5)	159 (2)
O(2)	x	2330 (3)	2329 (5)	2642 (7)	2754 (3)	6	B	3.4 (1)	4.5 (4)	9.8 (9)	4.1 (2)
8(j)	y	1213 (3)	1204 (4)	1123 (7)	1114 (3)	4(i)	Occ.	19 (1)	73 (2)	37 (1)	59 (1)
	z	6144 (8)	6158 (12)	6591 (17)	6708 (7)		x	210 (2)	226 (1)	228 (1)	226 (1)
	B	2.7 (1)	4.1 (2)	4.6 (3)	3.4 (1)		y	↓	↓	↓	↓
O(3)	x	1882 (3)	1858 (4)	1999 (6)	1999 (3)		z	-33 (5)	34 (1)	40 (3)	41 (1)
8(j)	y	1535 (3)	1476 (4)	1363 (6)	1375 (3)	7	B	4.6 (4)	4.8 (1)	6.0 (5)	4.2 (1)
	z	8902 (9)	8876 (11)	9007 (16)	8955 (7)	4(i)	Occ.	45 (1)			
	B	3.0 (1)	2.7 (2)	4.1 (3)	2.8 (1)		x	365 (1)			
O(4)	x	2304 (3)	2310 (4)	2345 (8)	2342 (3)		y	↓			
8(j)	y	1008 (3)	990 (4)	977 (7)	1005 (3)		z	334 (4)			
	z	2473 (8)	2501 (11)	2653 (18)	2673 (7)		B	6.7 (7)			
	B	2.5 (1)	3.3 (2)	5.6 (3)	3.1 (1)	8	Occ.	55 (2)			
O(5)	x	0	0	0	0	4(i)	x	419 (2)			
4(h)	y	3257 (5)	3273 (6)	2863 (12)	2598 (6)		y	↓			
	z	↓	↓	↓	↓		z	207 (4)			
	B	3.2 (2)	3.5 (2)	7.7 (6)	6.6 (2)		B	10.3 (8)			
O(6)	x	805 (3)	808 (4)	803 (6)	781 (3)	9	Occ.	49 (1)	24 (1)		
8(j)	y	1614 (3)	1574 (5)	1408 (6)	1437 (3)	4(i)	x	32 (1)	34 (2)		
	z	499 (8)	536 (12)	278 (16)	213 (7)		y	↓	↓		
	B	2.6 (1)	3.7 (2)	3.5 (2)	2.7 (1)		z	190 (2)	246 (4)		
O(7)	x	1226 (3)	1265 (5)	1402 (7)	1497 (3)		B	9.6 (3)	8.1 (6)		
8(j)	y	2296 (3)	2291 (5)	2167 (8)	2132 (3)	10	Occ.	100	89 (3)	65 (2)	81 (1)
	z	5515 (9)	5553 (13)	5487 (19)	5405 (8)	2(d)	x	0	0	0	0
	B	3.2 (1)	4.7 (2)	5.9 (3)	4.2 (1)		y	↓	↓	↓	↓
O(8)	x	142 (4)	116 (5)	228 (8)	281 (4)		z	↓	↓	↓	↓
8(j)	y	2709 (3)	2677 (4)	2531 (7)	2562 (3)		B	10.9 (7)	15.0 (12)	12.8 (8)	7.3 (2)
	z	1891 (9)	1872 (12)	1835 (20)	1883 (9)						
	B	3.4 (1)	3.9 (2)	6.6 (4)	4.3 (1)						
O(9)	x	2153 (3)	2127 (4)	2035 (6)	2036 (3)						
8(j)	y	2492 (3)	2495 (4)	2526 (6)	2504 (3)						
	z	1928 (8)	1793 (10)	1527 (15)	1473 (7)						
	B	2.4 (1)	2.8 (2)	3.1 (2)	2.5 (1)						
O(10)	x	1208 (3)	1233 (5)	1079 (7)	1049 (3)						
8(j)	y	3708 (3)	3695 (5)	3605 (7)	3594 (3)						
	z	4225 (9)	4211 (12)	4455 (18)	4651 (8)						
	B	2.8 (1)	4.0 (2)	5.0 (3)	3.6 (1)						

Correspondence of codes of extra-framework sites in (a) present work, (b) Alberti (1975), (c) Koyama & Takéuchi (1977)

(a)	(b)	(c)	(a)	(b)	(c)
1	H ₂ O (6)	W(6)	6	—	W(1)
2	C(3)	—	7	C(1)	M(1)
3	H ₂ O (3)	W(3)	8	H ₂ O (2)	W(2)
4	H ₂ O (5)	W(5)	9	C(2)	M(2)
5	H ₂ O (1)	M(3)	10	H ₂ O (4)	W(4)

form (I) indicates that there are also water molecules in addition to K at (1 + 2). The highest electron density was found in sites (5 + 6) (Fig. 2) and the refinement using the scattering function of potassium led to low B values and to a sum of the occupancy factors close to 100% in (I) and (II), and slightly higher B values and somewhat smaller occupancy factors in (III) and (IV).

Water molecules could only be found in sets (I) and (II). Considering the H_2O sites, site 3 is occupied 100% in (I) and about 50% in (II), while site 4 is occupied in (I) and (II) by 50% only, because it corresponds to two symmetry-equivalent positions too close to be occupied simultaneously. Sites 7 and 8 are close to each other and hence the sum of their occupancies cannot exceed 100%. Their electron densities disappear in set (II).

Set (I) favours the idea of the presence of potassium in site 9 and water in 10. For sets (III) and (IV) site 9 is empty and only site 10 is nearly fully occupied, obviously by potassium. Only in set (II) is the interpretation of sites 9 and 10 more critical. On the whole, we favour the idea of a progressive shift of potassium from site 9 to 10. It should be mentioned that reflection profiles in set (II) seem to indicate that the statistical distribution may not be constant over the whole single crystal.

As the attribution of the extra-framework sites to cations or to water molecules is always controversial in zeolites, it is useful to compare the present results only with the clinoptilolite data of Alberti (1975) and of Koyama & Takéuchi (1977), as these are the only refinements of alkali-rich zeolites with the heulandite framework; other heulandite structural data, for instance those of Merkle & Slaughter (1968), Alberti (1972), Bartl (1973), Bresciani-Pahor, Calligaris, Nardin, Randaccio & Russo (1980) and Bresciani-Pahor, Calligaris, Nardin & Randaccio (1981) can hardly be compared with our results because of the very different cation content. Anyway, the comparison with Alberti's (1975) and Koyama & Takéuchi's (1977) data is also only coarse, because K, dominant in our sample, is only a subordinate cation in the others. On the whole, in view of the fact that the total cation number is highest in our sample, the difference in the distribution of cations and water molecules is small, but it must be noted that site 7, attributed to water, corresponds to Alberti's $C(1)$ and to Koyama & Takéuchi's $M(1)$, both cation occupied, and the same is true for the analogous site in the natural and partially silver-exchanged heulandites studied by Bresciani-Pahor *et al.* (1980) and in the fully silver-exchanged heulandite studied by Bresciani-Pahor *et al.* (1981); in this case we strongly believe that site 7 is occupied by water only, because all electron density in the site has already disappeared at 373 K.

The positional and thermal parameters, the occupancy factors and the distribution of K^+ ions and water molecules of the extra-framework sites, as well as

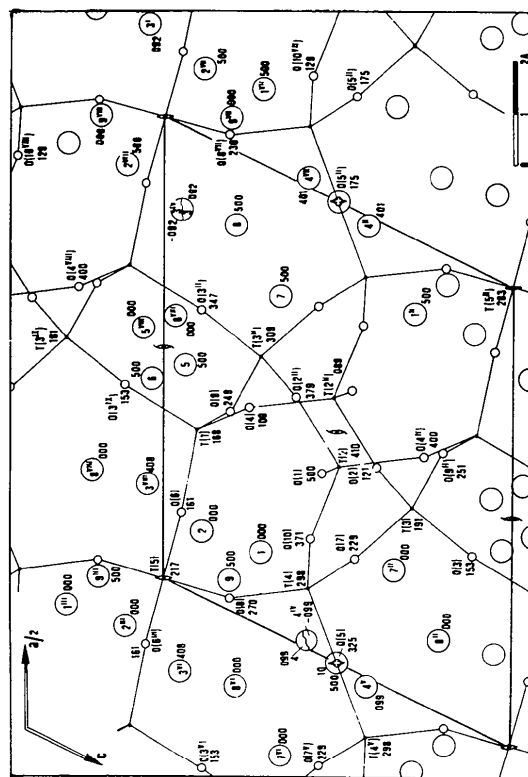


Fig. 3. Atomic positions of K-heulandite (I) (293 K) in the projection parallel to [010]. y parameters $\times 10^3$ are given with three-digit numbers. Framework atoms are connected with straight lines, extra-framework atoms are shown as large circles.

the correspondence of codes of extra-framework sites with natural heulandite, are given in Table 2 (see also Fig. 3). Using these values, the refinement was carried out to the final R factors listed in Table 1. Interatomic distances and angles of the framework are given in Table 3, interatomic distances (≤ 3.4 Å) of K^+ ions and water molecules to symmetry-equivalent positions, to extra-framework sites and to framework O atoms in Table 4.*

The silicate framework forms two channels of different sizes both at $y = 0$ and $y = \frac{1}{2}$ extending parallel to [001] (Fig. 4). The smaller one is confined by a ring of eight tetrahedra, the larger by a ring of ten tetrahedra. Since the Al distribution in the silicate framework is not changed when dehydrating the K-heulandite, average $T-O$ distances can be calculated for the five different framework tetrahedra $T(1) \dots T(5)$ of Table 3. The average $T-O$ distances of

* Lists of the complete set of all nearest neighbours around the extra-framework sites and structure factors have been deposited with the British Library Lending Division as Supplementary Publication No. SUP 38179 (63 pp.). Copies may be obtained through The Executive Secretary, International Union of Crystallography, 5 Abbey Square, Chester CH1 2HU, England.

Table 3. *Interatomic distances (Å) and angles (°) of the framework with e.s.d.'s on the last digit in parentheses*

	(I)	(II)	(III)	(IV)		(I)	(II)	(III)	(IV)
<i>T</i> (1) tetrahedron					<i>T</i> (4) tetrahedron				
<i>T</i> -O(3 ^h)	1-639 (6)	1-637 (7)	1-640 (12)	1-648 (5)	<i>T</i> -O(5)	1-631 (3)	1-629 (5)	1-557 (5)	1-579 (2)
-O(4)	1-630 (6)	1-625 (8)	1-637 (13)	1-617 (5)	-O(7)	1-621 (6)	1-637 (8)	1-560 (13)	1-611 (6)
-O(6)	1-639 (6)	1-637 (7)	1-627 (10)	1-653 (5)	-O(8)	1-616 (6)	1-623 (8)	1-652 (13)	1-603 (6)
-O(9)	1-615 (6)	1-609 (7)	1-659 (11)	1-626 (5)	-O(10)	1-609 (6)	1-643 (8)	1-576 (12)	4 (5)
Average	1-631 (11)	1-627 (13)	1-641 (13)	1-636 (17)	Average	1-619 (9)	1-633 (9)	1-586 (45)	1-599 (14)
O(3 ^h)- <i>T</i> -O(4)	105.3 (3)	105.3 (4)	103.6 (6)	106.8 (3)	O(5)- <i>T</i> -O(7)	110.5 (3)	112.9 (4)	113.9 (8)	110.6 (3)
-O(6)	108.4 (3)	108.6 (4)	108.8 (6)	108.6 (3)	-O(8)	107.8 (3)	108.9 (3)	109.0 (5)	107.6 (2)
-O(9)	112.3 (3)	112.4 (4)	111.3 (6)	110.1 (2)	-O(10)	105.8 (4)	106.0 (5)	103.7 (9)	110.4 (4)
O(4)- <i>T</i> -O(6)	108.2 (3)	106.5 (4)	104.8 (6)	106.5 (3)	O(7)- <i>T</i> -O(8)	109.3 (3)	110.1 (4)	110.5 (7)	109.7 (3)
-O(9)	112.1 (3)	114.0 (4)	115.1 (6)	114.0 (3)	-O(10)	113.8 (3)	109.2 (4)	111.1 (7)	110.3 (3)
O(6)- <i>T</i> -O(9)	110.3 (3)	109.8 (4)	112.5 (6)	110.6 (2)	O(8)- <i>T</i> -O(10)	109.6 (3)	109.8 (4)	108.2 (7)	108.1 (3)
<i>T</i> (2) tetrahedron					<i>T</i> (5) tetrahedron				
<i>T</i> -O(1)	1-641 (3)	1-638 (4)	1-617 (6)	1-642 (3)	<i>T</i> -O(6) [×2]	1-651 (6)	1-653 (8)	1-642 (10)	1-631 (5)
-O(2 ^h)	1-653 (6)	1-667 (8)	1-640 (12)	1-657 (5)	-O(8) [×2]	1-629 (6)	1-614 (8)	1-572 (13)	1-586 (6)
-O(4 ^h)	1-669 (6)	1-673 (8)	1-671 (12)	1-650 (5)	Average	1-640 (13)	1-633 (22)	1-607 (40)	1-608 (26)
-O(10)	1-665 (6)	1-593 (8)	1-631 (11)	1-653 (5)	O(6)- <i>T</i> -O(6 ^h)	105.2 (4)	104.2 (6)	108.0 (8)	106.1 (4)
Average	1-657 (13)	1-643 (36)	1-640 (23)	1-650 (6)	-O(8) [×2]	111.9 (3)	112.7 (4)	112.6 (6)	111.5 (3)
O(1)- <i>T</i> -O(2 ^h)	107.8 (4)	107.8 (5)	108.3 (8)	108.5 (3)	-O(8 ^h) [×2]	110.2 (3)	109.2 (4)	110.2 (6)	111.7 (3)
-O(4 ^h)	109.3 (4)	110.7 (5)	106.4 (7)	108.8 (3)	O(8)- <i>T</i> -O(8 ^h)	107.6 (5)	108.9 (6)	103.3 (10)	104.5 (4)
-O(10)	106.6 (3)	105.5 (5)	106.4 (7)	104.7 (3)	<i>T</i> -O- <i>T</i>				
O(2 ^h)- <i>T</i> -O(4 ^h)	110.7 (3)	109.7 (4)	111.4 (6)	112.5 (3)	<i>T</i> (1)-O(6)- <i>T</i> (5)	137.9 (4)	136.2 (5)	131.5 (7)	132.2 (3)
-O(10)	110.8 (3)	111.1 (4)	112.6 (7)	112.0 (3)	-O(3 ^h)- <i>T</i> (3 ^h)	145.1 (4)	140.2 (5)	136.2 (8)	138.5 (3)
O(4 ^h)- <i>T</i> -O(10)	111.5 (3)	111.9 (4)	111.4 (7)	110.1 (3)	-O(4)- <i>T</i> (2 ^h)	136.5 (4)	136.9 (5)	143.2 (9)	146.4 (3)
<i>T</i> (3) tetrahedron					-O(9)- <i>T</i> (3 ^h)	150.5 (4)	149.3 (5)	148.8 (7)	152.1 (3)
<i>T</i> -O(2)	1-621 (6)	1-614 (8)	1-626 (12)	1-647 (5)	<i>T</i> (2)-O(1)- <i>T</i> (2 ^h)	154.8 (5)	148.9 (7)	147.9 (10)	144.0 (5)
-O(3)	1-633 (6)	1-648 (7)	1-663 (12)	1-647 (5)	-O(2 ^h)- <i>T</i> (3 ^h)	148.7 (4)	148.6 (6)	144.3 (8)	141.9 (3)
-O(7)	1-632 (6)	1-571 (8)	1-638 (12)	1-603 (6)	-O(10)- <i>T</i> (4)	148.0 (4)	151.2 (6)	144.9 (8)	139.8 (3)
-O(9 ^h)	1-625 (5)	1-667 (7)	1-595 (10)	1-623 (5)	<i>T</i> (3)-O(7)- <i>T</i> (4)	154.3 (4)	158.9 (6)	157.5 (9)	152.4 (4)
Average	1-628 (6)	1-625 (42)	1-630 (28)	1-630 (21)	<i>T</i> (4)-O(5)- <i>T</i> (4 ^h)	144.8 (6)	141.1 (8)	167.8 (16)	164.6 (7)
O(2)- <i>T</i> -O(3)	104.3 (3)	102.9 (4)	101.2 (6)	103.5 (3)	-O(8)- <i>T</i> (5)	152.4 (4)	151.8 (5)	154.2 (9)	151.8 (4)
-O(7)	109.4 (3)	108.9 (5)	109.0 (7)	108.7 (3)	<i>T</i> - <i>T</i> - <i>T</i>				
-O(9 ^h)	110.9 (3)	110.4 (4)	110.5 (6)	110.9 (3)	<i>T</i> (5 ^h)- <i>T</i> (5)- <i>T</i> (5 ^h)	164.7 (1)	163.6 (1)	155.7 (2)	157.2 (1)
O(3)- <i>T</i> -O(7)	108.2 (3)	110.3 (4)	110.8 (6)	112.9 (3)					
-O(9 ^h)	112.1 (3)	112.6 (4)	112.1 (6)	110.4 (2)					
O(7)- <i>T</i> -O(9 ^h)	111.7 (3)	111.3 (4)	112.8 (7)	110.3 (3)					

Symmetry code: (i) $1-x, y, -z$; (ii) $\frac{1}{2}-x, \frac{1}{2}-y, 1-z$; (iii) $-x, y, -z$; (iv) $x, -y, z$; (v) $-x, y, 1-z$; (vi) $x-\frac{1}{2}, \frac{1}{2}-y, z$; (vii) $\frac{1}{2}+x, \frac{1}{2}-y, z$; (viii) $\frac{1}{2}-x, \frac{1}{2}-y, -z$; (ix) $x, y, z-1$; (x) $x, 1-y, z$; (xi) $x-\frac{1}{2}, \frac{1}{2}-y, z-1$.

Table 4. *Unique distances (≤ 3.4 Å) in polyhedra*

Distances between positions statistically occupied and corresponding to unacceptable contacts are omitted.

	(I)	(II)	(III)	(IV)		(I)	(II)	(III)	(IV)
1-O(4)	3.35 (3)	3.29 (1)	3.12 (3)	3.08 (1)	4-O(7 ^h)	3.38 (2)	—	—	—
-O(6)	3.38 (2)	3.20 (1)	2.75 (2)	2.79 (1)	-4 ^{iv}	—	3.18 (4)	—	—
-1 ⁱⁱⁱ	—	—	2.90 (7)	2.91 (3)	-7 ⁱⁱ	2.84 (2)	—	—	—
-2 ⁱⁱⁱ	2.95 (4)	2.33 (1)	—	—	-7 ^{vi}	2.94 (2)	—	—	—
-4	2.61 (3)	2.34 (1)	—	—	-8 ⁱⁱ	3.10 (3)	—	—	—
-7 ⁱⁱ	2.59 (5)	—	—	—	-8 ^{vi}	2.43 (2)	—	—	—
-8 ^{vi}	2.64 (3)	—	—	—	5-O(1)	3.35 (1)	3.40 (2)	3.36 (4)	—
2-O(4)	3.14 (1)	—	—	—	-O(2 ^h)	3.13 (1)	3.01 (2)	2.52 (2)	2.54 (1)
-O(6)	2.95 (1)	3.01 (1)	2.94 (5)	2.76 (1)	-O(3 ^h)	2.98 (1)	2.73 (1)	2.52 (2)	2.56 (1)
-O(6 ⁱⁱⁱ)	—	3.24 (1)	2.64 (4)	2.92 (1)	-O(4 ^{vi})	3.13 (1)	3.14 (2)	—	—
-2 ⁱⁱⁱ	2.32 (3)	—	—	—	-7	2.25 (2)	—	—	—
-4	—	2.81 (2)	—	—	-8	2.85 (3)	—	—	—
-8 ^{vi}	3.08 (3)	—	—	—	6-O(1)	—	3.36 (1)	—	—
-8 ^{vi}	2.44 (3)	—	—	—	-O(2 ^h)	—	3.19 (1)	2.91 (2)	2.88 (1)
3-O(5 ⁱⁱ)	3.36 (1)	—	—	—	-O(3 ^h)	3.21 (2)	2.97 (1)	2.62 (1)	2.65 (1)
O(8 ^{vi})	3.00 (1)	2.93 (3)	—	—	-O(4 ^{vi})	2.91 (2)	3.09 (1)	3.12 (2)	3.19 (1)
-O(10 ^{viii})	—	3.33 (3)	—	—	-7	2.91 (4)	—	—	—
-O(10 ^{viii})	3.38 (1)	3.17 (3)	—	—	-8	3.35 (4)	—	—	—
3 ⁱ	—	2.36 (5)	—	—	7-O(2 ^h)	2.92 (2)	—	—	—
-3 ^{iv}	3.31 (2)	2.94 (6)	—	—	-O(3 ^h)	3.14 (1)	—	—	—
-5 ^{viii}	2.92 (1)	—	—	—	8-O(3 ^h)	3.25 (1)	—	—	—
-6 ^{viii}	2.62 (2)	3.13 (3)	—	—	9-O(1)	2.74 (1)	2.49 (3)	—	—
-9 ^{vii}	2.59 (1)	2.24 (3)	—	—	-O(10)	2.91 (1)	2.78 (2)	—	—
-9 ^{viii}	2.94 (1)	2.75 (3)	—	—	-9 ⁱⁱⁱ	2.54 (1)	3.31 (5)	—	—
4-O(3 ^y)	3.36 (2)	3.33 (3)	—	—	-10	2.61 (1)	2.22 (3)	—	—
-O(6)	—	3.37 (2)	—	—	10-O(1)	—	—	3.06 (1)	2.88 (1)
-O(6 ⁱⁱⁱ)	3.29 (2)	3.12 (2)	—	—	-O(5)	3.13 (1)	3.06 (1)	—	—
-O(7)	2.97 (2)	3.10 (2)	—	—	-O(10)	3.38 (1)	—	3.20 (1)	3.13 (1)

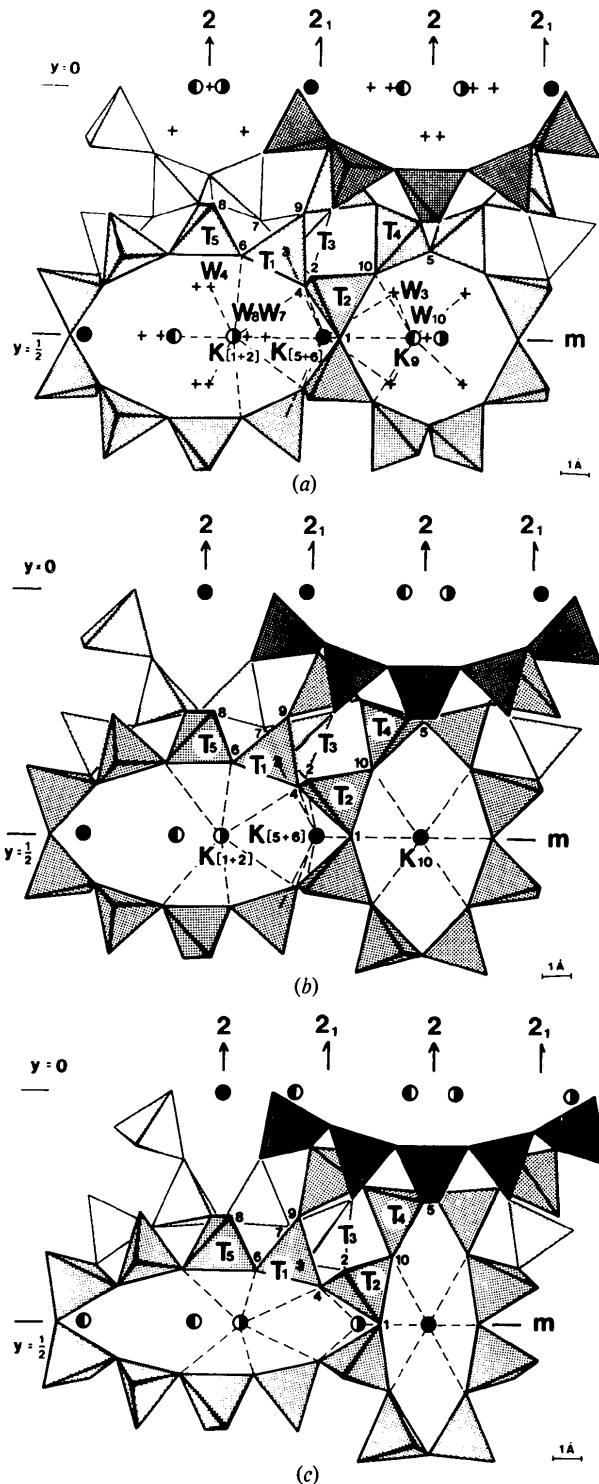


Fig. 4. Projections of the framework tetrahedra parallel to [001]. At the left the larger channel (A), at the right the smaller channel (B). Coordinations of the extra-framework atoms are given by dotted lines. (a) Fully hydrated K-heulandite ($\text{Na}_{0.10}\text{K}_{8.57}\text{Ba}_{0.04}(\text{Al}_{9.31}\text{Si}_{26.83}\text{O}_{72}) \cdot 19.56\text{H}_2\text{O}$). (b) Dehydrated K-heulandite ($\text{Na}_{0.10}\text{K}_{8.57}\text{Ba}_{0.04}(\text{Al}_{9.31}\text{Si}_{26.83}\text{O}_{72})$). (c) Dehydrated (at 613 K for 60 h) natural heulandite ($\text{Na}_{1.26}\text{K}_{0.43}\text{Mg}_{0.01}\text{Ca}_{3.57}\text{Sr}_{0.05}\text{Ba}_{0.06}(\text{Al}_{9.37}\text{Si}_{26.70}\text{O}_{72}) \cdot 26 \cdot \text{OH}_2\text{O}$ (Alberti, 1973)).

sets (I)–(IV) from $T(1) \dots T(5)$ are 1.634 (14), 1.647 (21), 1.628 (23), 1.609 (55), 1.622 (30) Å. The average T –O distances indicate that the highest share of Al occurs in $T(2)$, the lowest in $T(4)$. Because of the statistical Al distribution in the silicate framework for the space group $C2/m$ is to be considered statistically, and the negative net-charge distribution in the framework remains preserved upon dehydration. This distribution is particularly concentrated along the channel walls between the eight-membered-ring and ten-membered-ring channels parallel to (100). The probability of the distribution of K^+ ions is highest in those sites where the negative charge density is high and the K^+ ions are as distant from each other as possible; therefore in all four sets the K^+ ions lie statistically distributed in the mirror plane.

In the dehydrated forms (III) and (IV), $\text{K}(5+6)$ are fixed on the channel walls, $\text{K}(1+2)$ in the large channel and $\text{K}(10)$ in the small channel (Fig. 2*b,d*); they are six-coordinated almost planar and/or in the form of a flat pyramid (Fig. 5).

The results of the diffraction data sets (III) and (IV) are very similar. The electron density maps (Fig. 2*b,d*) show essentially no difference in the K^+ sites and only the maxima of set (III) have more elongated shapes. This experiment indicates that the structural results obtained by dehydration of zeolites at high tempera-

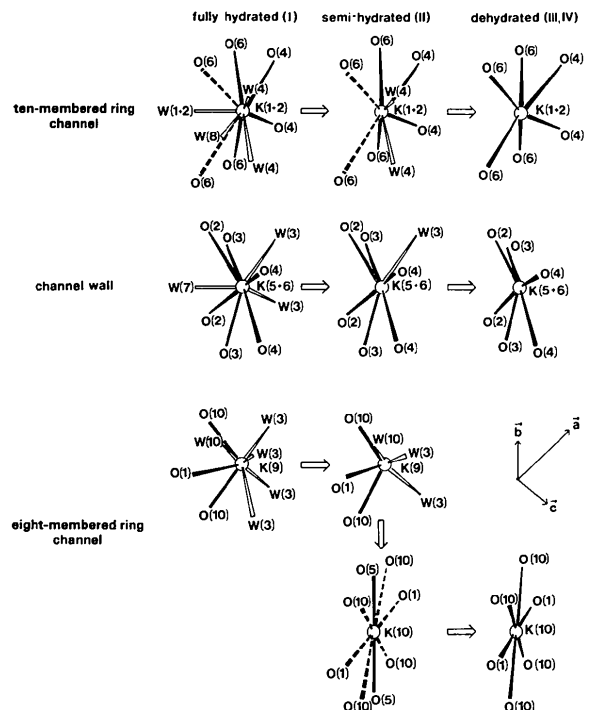


Fig. 5. Change of the K^+ ion coordination during dehydration of K-heulandite. The full-lined coordinations are ≤ 3.4 Å, the dotted lines show distances > 3.4 Å.

tures are similar to those obtained at room temperature after sealing in a glass capillary.

In the fully hydrated form (I) all water molecules (3, 4, 7/8, 10 and partly 1 + 2) lie in the channels: $W(3)$ and $W(10)$ lie in the eight-membered-ring channel, $W(4)$, $W(7/8)$ and 1 + 2 in the ten-membered-ring channel (Fig. 4a). Each of the water molecules is bonded to one or two K^+ ions and to O atoms of the silicate framework. All K^+ ions are coordinated by water molecules and O atoms of the silicate framework (Fig. 5). $K(5 + 6)$ is fixed at the channel wall, $K(1 + 2)$ in the larger channel and $K(9)$ at the smaller channel.

In the semi-hydrated form (II) the water molecules 7/8 and 1 + 2 are lost as well as half of $W(3)$ and $W(10)$. Each of these remaining water molecules is bonded to one K^+ ion and to O atoms of the silicate framework. $K(5 + 6)$ is fixed at the channel wall, $K(1 + 2)$ in the larger channel. In the smaller channel one part of the potassium, $K(9)$, is coordinated by silicate O atoms and water molecules, the other part, $K(10)$, is coordinated only by framework O atoms (Fig. 5).

Discussion

Alietti, Gottardi & Poppi (1974) showed that a natural Ca-rich heulandite, which is subjected to a strong reduction of the unit-cell dimensions when heated at 573 K, features a different behaviour when exchanged with rubidium and potassium. The Rb-exchanged form does not show any cell contraction at all, whereas the K-exchanged form exhibits a 2% contraction of b at 673 K with a heating rate of 10 K min^{-1} ; when cooled to room temperature after heating, it maintains the contraction, at least in part. The data of set (IV) (Table 1) show a contraction of b by 3.4%, of a by 1.6% and of c by 0.3%. There is only a 5.6% reduction of the cell volume for K-heulandite, whereas a Ca-rich heulandite shows a 15% reduction of volume under the same temperature conditions (Alberti, 1973).

Since there is a change in cell volume or shape, there is also one in the framework. The angle $T(5^{xl})-T(5)-T(5^{ll})$ was assumed by Alberti (1973) as an index for the deformation of the framework; so for the Ca-rich heulandite at room temperature the angle is 162° and after heating and cooling is 147° . In the K-exchanged sample, the angle in (I) is 165° and in (IV) 157° . So both cell-volume reduction and framework deformation are less than half in comparison to the Ca-rich form.

The spatial shifts of the $T(\text{Si,Al})$ position within the framework on heating are smaller than 0.4 \AA . The $T-O$ distances on heating do not change considerably either (Table 3). In the dehydration sets (III, IV) the O atoms O(1) and O(5) of the framework show the largest changes ($\sim 0.8 \text{ \AA}$). This fairly large change is

Table 5. Channel sizes (\AA) of the ten-membered-ring (A) and the eight-membered-ring (B)

Channel	K-heulandite (this work)		Natural heulandite (Alberti, 1973)	
	A	B	A	B
Fully hydrated	9.6×5.8	6.4×6.2	9.6×5.7	6.3×6.2
		(Fig. 4a)		
Semi-hydrated	9.9×5.6	6.0×6.15		
Dehydrated	10.7×5.0	4.95×8.4	11.5×3.8	3.5×9.4
		(Fig. 4b)		(Fig. 4c)

mainly related to the change of potassium from site 9 to 10. The silicate framework in natural heulandites, clinoptilolites, exchanged K-heulandite and dehydrated heulandites is characterized by ten-membered-ring (A) and eight-membered-ring (B) channels. The shape of the channels in the dehydrated state is a function of the size and amount of the cations. It is more deformed at smaller size and/or smaller amount of cations (Table 5). In the fully hydrated form (I) and semi-hydrated form (II) the smaller channel (B) has a nearly circular cross-section (Fig. 4a), while in the dehydrated forms (III and IV) it attains a shape which is more elongated parallel to $[010]$ (Fig. 4b).

Fig. 4(c) shows the same projection of the dehydrated natural heulandite (heulandite B, Alberti, 1973). The smaller size and the amount of the cations cause a much stronger deformation of the silicate framework. Both dehydrated forms (III) and (IV) as well as heulandite B could be rehydrated to the corresponding fully hydrated heulandites.

During the dehydration of heulandites the silicate framework does not collapse, but is only deformed depending on the size and amount of the cations within the channels. The process of dehydration takes place in two steps by loss of the water molecules and change of potassium in channel B from position $K(9)$ to $K(10)$. In the semi-hydrated form (II) one half of the water is lost and one half of the potassium in channel B occupies $K(9)$ and the other half $K(10)$. In the dehydrated forms (III, IV) in channel B the K^+ ions occupy only $K(10)$. The change of coordination of K^+ ions during the dehydration process is shown in Fig. 5.

The process of dehydration is accompanied by a deformation of the silicate framework. If the channels are no longer filled with enough water molecules the silicate framework begins to deform.

This work was made possible through the financial support of the 'Fonds zur Förderung der wissenschaftlichen Forschung in Österreich' (project Nos. 2178 and 2365) and the Consiglio Nazionale delle Ricerche, Roma. The SiO_2 -glass tube was produced for us by the Max-Planck-Institut für Festkörperforschung in Stuttgart. For the construction of the heating equipment we thank B. Branka and Doz Dr H.

Völlenklee. Thanks are due also to the Centro di Cristallografia Strutturale del CNR di Pavia for recording the counter data of sample (IV). All calculations were carried out at the Centro di Calcolo dell'Università di Modena.

References

- ALBERTI, A. (1972). *Tschermaks Mineral. Petrogr. Mitt.* **18**, 129–146.
- ALBERTI, A. (1973). *Tschermaks Mineral. Petrogr. Mitt.* **19**, 173–184.
- ALBERTI, A. (1975). *Tschermaks Mineral. Petrogr. Mitt.* **22**, 25–37.
- ALIETTI, A., GOTTARDI, G. & POPPI, L. (1974). *Tschermaks Mineral. Petrogr. Mitt.* **21**, 291–298.
- BARTL, H. (1973). *Z. Kristallogr.* **137**, 440–441.
- BRESCIANI-PAHOR, N., CALLIGARIS, M., NARDIN, G. & RANDACCIO, L. (1981). *J. Chem. Soc. Dalton Trans.* pp. 2288–2291.
- BRESCIANI-PAHOR, N., CALLIGARIS, M., NARDIN, G., RANDACCIO, L. & RUSSO, E. (1980). *J. Chem. Soc. Dalton Trans.* pp. 1511–1514.
- BUSING, W. R., MARTIN, K. O. & LEVY, H. A. (1962). *ORFLS Report ORNL-TM-305*. Oak Ridge National Laboratory, Tennessee.
- HAJDÚ, F. (1972). *Acta Cryst.* **A28**, 250–252.
- HANSON, H. P., HERMAN, F., LEA, J. D. & SKILLMAN, G. (1964). *Acta Cryst.* **17**, 1040–1044.
- KOYAMA, K. & TAKÉUCHI, Y. (1977). *Z. Kristallogr.* **145**, 216–239.
- MERKLE, A. B. & SLAUGHTER, M. (1968). *Am. Mineral.* **53**, 1120–1138.
- PASSAGLIA, E., PONGILUPPI, D. & VEZZALINI, G. (1978). *Neues Jahrb. Mineral. Monatsh.* pp. 310–324.

Acta Cryst. (1983). **B39**, 197–209

A Transmission Electron Microscopical Study of the σ Phase in an Iron–Chromium Steel

BY P. G. SELF*

Department of Metallurgy and Materials Science, University of Cambridge, Cambridge, England

M. A. O'KEEFE

High Resolution Electron Microscope, Free School Lane, University of Cambridge, Cambridge, England

AND W. M. STOBBS

Department of Metallurgy and Materials Science, University of Cambridge, Cambridge, England

(Received 20 October 1981; accepted 19 October 1982)

Abstract

This paper details several aspects of the σ phase in a duplex stainless steel. The growth and morphology of the phase is characterized and it is demonstrated that under certain conditions the nature of the nucleation and growth produces faulting within the σ -phase particles. The crystalline structure of the phase is discussed with reference to the possibility that it might be that of β -uranium rather than that previously reported. In this connection a comparison is made of the relative usefulness of high resolution and various indirect methods for analysing the structure. In particular, the absences in diffraction patterns and their

dependence on crystal tilt and thickness offer an insight into the requirements for accurate structure determination by high-resolution electron microscopy. Finally, the fault structure is examined and a planar (110)-type fault is discussed in detail.

1. Introduction

The σ phase arises in a number of binary and also ternary transition-metal alloy systems. It is of interest technologically in that its formation in high-alloy steels, based on the Fe–Cr system, tends to lead to embrittlement. This is essentially because, once nucleated, σ -phase particles can grow to relatively large sizes and are particularly hard; the sequence faults they typically contain not being easily sheared. The phase is of

* Presently at Department of Geology, Arizona State University, Tempe, Arizona, USA.